Human Genetics (2019) 138:625–634
https://doi.org/10.1007/s00439-019-02011-x

ORIGINAL INVESTIGATION

Biallelic variants in *SMAD6* are associated with a complex cardiovascular phenotype

Katja Kloth[1] · Tatjana Bierhals[1] · Jessika Johannsen[2] · Frederike L. Harms[1] · Jane Juusola[3] · Mark C. Johnson[4] · Dorothy K. Grange[5] · Kerstin Kutsche[1]

Received: 26 February 2019 / Accepted: 3 April 2019 / Published online: 8 April 2019

Abstract

Rare heterozygous variants in *SMAD6* have been identified as a significant genetic contributor to bicuspid aortic valve-associated thoracic aortic aneurysm on one hand and non-syndromic midline craniosynostosis on the other. In this study, we report two individuals with biallelic missense variants in *SMAD6* and a complex cardiac phenotype. Trio exome sequencing in Proband 1, a male who had aortic isthmus stenosis, revealed the homozygous *SMAD6* variant p.(Ile466Thr). He also had mild intellectual disability and radio-ulnar synostosis. Proband 2 is a female who presented with a more severe cardiac phenotype with a dysplastic and stenotic pulmonary valve and dilated cardiomyopathy. In addition, she had vascular anomalies, including a stenotic left main coronary artery requiring a bypass procedure, narrowing of the proximal left pulmonary artery and a venous anomaly in the brain. Proband 2 has compound heterozygous *SMAD6* missense variants, p.(Phe357Ile) and p.(Ser483Pro). Absence of these *SMAD6* variants in the general population and high pathogenicity prediction scores suggest that these variants caused the probands' phenotypes. This is further corroborated by cardiovascular anomalies and appendicular skeletal defects in *Smad6*-deficient mice. SMAD6 acts as an inhibitory SMAD and preferentially inhibits bone morphogenetic protein (BMP)-induced signaling. Our data suggest that biallelic variants in *SMAD6* may affect the inhibitory activity of SMAD6 and cause enhanced BMP signaling underlying the cardiovascular anomalies and possibly other clinical features in the two probands.

Introduction

Bicuspid aortic valve (BAV) is the most common form of congenital heart disease, affecting 0.5–2% of the general adult population (Braverman et al. 2005; Friedman et al. 2008; Gillis et al. 2017; Malcic et al. 2015), although necropsy studies suggest the true incidence of BAV may still be underestimated in the general population (Girdauskas and Borger 2013). BAV describes an anatomical anomaly of the aortic valve which is formed of two cusps instead of three, thus leading to stenosis or insufficiency of the valve as well as development of an enlarged aorta due to aortic valve regurgitation (Friedman et al. 2008; Girdauskas and Borger 2013). This condition correlates with a 20% risk of developing thoracic aortic aneurysm (TAA) (Gillis et al. 2017; Hinton 2012; Lewin and Otto 2005; Tzemos et al. 2008; Vallely et al. 2008). Familial occurrence of BAV suggests an autosomal dominant inheritance with reduced penetrance and variable expressivity (Braverman et al. 2005; Vallely et al. 2008). Sequence variants in a few genes have been linked to BAV, either

Electronic supplementary material The online version of this article (https://doi.org/10.1007/s00439-019-02011-x) contains supplementary material, which is available to authorized users.

✉ Kerstin Kutsche
kkutsche@uke.de

1 Institute of Human Genetics, University Medical Center Hamburg-Eppendorf, Martinistraße 52, 20246 Hamburg, Germany

2 Department of Pediatrics, University Medical Center Hamburg-Eppendorf, Hamburg, Germany

3 GeneDx, Gaithersburg, MD, USA

4 Division of Pediatric Cardiology, Department of Pediatrics, Washington University School of Medicine/St. Louis Children's Hospital, St. Louis, MO, USA

5 Division of Genetics and Genomic Medicine, Department of Pediatrics, Washington University School of Medicine/St. Louis Children's Hospital, St. Louis, MO, USA

as an isolated finding or with additional cardiovascular anomalies, including *NOTCH1, SMAD6*, and *MAT2A* (Garg et al. 2005; Gillis et al. 2017; Guo et al. 2015; Tan et al. 2012). The recent identification of heterozygous *SMAD6* missense and frameshift variants and one *in-frame* deletion suggested a significant contribution of loss-of-function (LOF) variants in this gene to the BAV/TAA phenotype. *SMAD6* encodes a member of the inhibitory SMADs (I-SMAD); SMAD6 preferentially inhibits SMAD signaling by bone morphogenetic protein (BMP) type I receptors (Goto et al. 2007). Pathogenic amino acid substitutions are located in the functionally important MH1 or MH2 domain of SMAD6 (Gillis et al. 2017; Tan et al. 2012). The MH1 domain has been shown to bind to DNA (Bai and Cao 2002). In addition to SMAD6's ability to directly bind to DNA, interaction of SMAD6 with transcriptional co-repressors and transcription factors in the nucleus indicates a function of this I-SMAD in an antagonistic feedback loop of the BMP signaling pathway (Bai et al. 2000; Lin et al. 2003; Miyazawa and Miyazono 2017).

Interestingly, another set of rare heterozygous LOF and missense variants in *SMAD6* has been detected in patients with isolated midline craniosynostosis (Timberlake et al. 2016, 2017). Penetrance of about 60% in individuals carrying a *SMAD6* variant revealed that additional risk factors must contribute to the development of this condition. A common variant near *BMP2* together with the *SMAD6* variant were found to account for cases with craniosynostosis and suggested a two-locus inheritance of this congenital malformation (Timberlake et al. 2016). Overall, these data imply that the *SMAD6* alleles associated with BAV/TAA in combination with other (common) variants produce the genotypes with high penetrance in this cohort of patients with cardiovascular complications. Of note, overlapping skeletal and cardiac phenotypes have not yet been reported.

In this study, we report two patients harboring biallelic variants in *SMAD6* identified by trio exome sequencing. Both presented with congenital heart and vascular defects affecting the cardiac valves, the aorta, cerebral and/or coronary vessels as well as facial dysmorphism.

Materials and methods

Study approval

Informed consent for genetic analyses was obtained from the two subjects, and genetic studies were performed clinically or as approved by the Hamburg Medical Chamber (reference number PV3802). Permission to publish photographs was provided for both probands.

Exome sequencing, data analysis, and variant validation

Genomic DNA was extracted from peripheral blood samples using standard procedures. Trio whole-exome sequencing (trio WES) with DNA samples of Proband 1 and both healthy parents was performed as described before (Hempel et al. 2015; Rauch et al. 2012). Briefly, coding DNA fragments were enriched with the SureSelect Human All Exon 50MbV5 Kit (Agilent), and captured libraries were then loaded and sequenced on the HiSeq2500 platform (Illumina). Reads were aligned to the human reference genome (UCSC GRCh37/hg19) using the Burrows–Wheeler Aligner (BWA, v.0.5.87.5), and detection of genetic variation was performed with SAMtools (v.0.1.18), PINDEL (v. 0.2.4t), and ExomeDepth (v.1.0.0).

Sequence validation and segregation analysis of all candidate variants in Proband 1 and his parents were performed by Sanger sequencing. Primer pairs designed to amplify selected coding exons of *SMAD6* and PCR conditions are available on request. Amplicons were directly sequenced using the ABI BigDye Terminator Sequencing kit (Applied Biosystems) and an automated capillary sequencer (ABI 3500, Applied Biosystems). Sequence electropherograms were analyzed using the Sequence Pilot software (JSI Medical Systems).

Using genomic DNA from Proband 2 and parents, the exonic regions and flanking splice junctions of the genome were captured using the SureSelect Human All Exon V4 Kit (50 Mb). Massively parallel (NextGen) sequencing was done on an Illumina system with 100 bp or greater paired-end reads. Reads were aligned to human genome build GRCh37/UCSC hg19 and analyzed for sequence variants using a custom-developed analysis tool. Additional sequencing technology and variant interpretation protocol have been previously described (Retterer et al. 2016). The general assertion criteria for variant classification are publicly available on the GeneDx ClinVar submission page (http://www.ncbi.nlm.nih.gov/clinvar/submitters/26957/).

RNA isolation, cDNA synthesis, cloning and colony PCR

Total RNA was extracted (PAXgene Blood RNA kit, PreAnalytiX) from a PAXgene blood sample of Proband 2 according to the manufacturer's instructions. 1 µg total RNA was reverse transcribed (Superscript™ III RT, ThermoFisher) using random hexamers as primers, and 1 µl of the reverse transcription reaction was utilized to amplify a 693-bp *SMAD6* cDNA fragment encompassing the c.1069T > A and c.1447T > C variants (forward primer

[located in exon 1]: 5′-TGCAACCCCTACCACTTCAG-3′; reverse primer [located in exon 4]: 5′-GAGGATCTCCAG CCAGCAG-3′). The PCR product was cloned into the pCR2.1 TOPO TA Cloning Vector (ThermoFisher). Individual *E. coli* clones were subjected to colony PCR followed by Sanger sequencing for haplotype determination.

Results

Clinical reports

Proband 1

The German proband is the first child of healthy, consanguineous South Asian parents (cousins 1°). Family history was unremarkable except for his 3-year-old brother who presented with mild speech delay. Clinical data are summarized in Table 1. The pregnancy had been complicated by maternal hypertension. Prenatal ultrasound revealed IUGR, abnormal head shape and suspicion of a subependymal hemorrhage. He was born via cesarean section at 35 weeks and 4 days. Measurements at birth were unremarkable: weight 2.140 g (− 1.39 *z*), length 44 cm (− 1.72 *z*), head circumference 31 cm (− 1.56 *z*). Postnatally, he presented with muscular hypotonia and recurrent hypoglycemic episodes. An echocardiogram showed mild aortic isthmus stenosis, and ultrasound of the abdomen revealed unilateral renal hypoplasia. X-ray confirmed a radio-ulnar synostosis and bilateral syndactyly of toes II/III. Facial dysmorphism and hirsutism were noted. His motor development was slightly delayed (sitting at 8 months, crawling at 10 months, walking at 19 months), and he started to speak at 24 months. His teething, hearing and vision were unremarkable. At last follow-up, he was 6 years old and had normal measurements: weight 21 kg (− 0.46 *z*), length 122 cm (+ 0.26 *z*), head circumference 50 cm (− 1.76 *z*). He had mild to moderate development delay. Cardiac MRI showed an aortic isthmus stenosis with a suspected tricuspid aortic valve. He also has intermittent (extra-)ventricular systoles. EEG revealed a dysrhythmic pattern without seizure activity. Craniofacial dysmorphism included deep-set and slightly posteriorly rotated ears, bushy eyebrows, downslanting palpebral fissures, long nasal bridge and prominent columella (Fig. 1a, b). Brain MRI was normal and previous genetic testing including routine karyotyping and chromosome microarray analysis was unremarkable.

Proband 2

The American proband is the first child of healthy nonconsanguineous Caucasian parents. Her family history was unremarkable. Clinical data are summarized in Table 1. Pregnancy was uneventful, and she was born at term. Her birth measurements were normal: weight 3.465 g (− 0.02 *z*) and length 49.5 cm (− 1 *z*) (head circumference not documented). Postnatally, she presented with a patent urachus that closed spontaneously. She had a heart murmur due to pulmonary valve stenosis diagnosed by echocardiogram. She required a balloon valvuloplasty at 6 months of age. She had a small to moderate secundum atrial septal defect that closed spontaneously. She developed evidence of a dilated cardiomyopathy with dilated left ventricle and mildly decreased systolic function for several years after that, and she was treated with the ACE inhibitor enalapril, but this gradually improved and medication was discontinued at age 7 years.

Her motor and speech development was unremarkable (sitting at 6 months, crawling at 10 months, walking at 15 months); her cognitive function is normal. She has never had seizures and no EEG was recorded. She has complained of headaches. Brain MRI showed enlargement and engorgement of some internal cerebral veins and sinuses. MR angiogram showed a persistent fetal/embryonic venous channel extending from the superior to the inferior sagittal sinus, but there was no evidence of a vascular malformation. Her hearing and vision are normal and an abdominal ultrasound was unremarkable. Laboratory studies revealed neutropenia and hypogammaglobulinemia, but additional immunological studies were normal, and the abnormalities eventually normalized. She had obstructive sleep apnea that improved following tonsillectomy and adenoidectomy.

At 10 years of age, she presented with a 6-month history of worsening chest pain, dyspnea on exertion and exercise intolerance. On cardiac catheterization, she was found to have severe left main coronary artery stenosis (99% occlusion with collateralization). Cardiac MRI reported a dysplastic pulmonic valve and mild narrowing of the proximal left pulmonary artery at the bifurcation. The left main coronary artery was severely narrowed and arose from the posterior aspect of the left coronary cusp before taking an acute angle with a slit-like configuration. She underwent an unsuccessful attempt to stent the artery and then required one vessel coronary artery bypass surgery with a left internal mammary artery to left anterior descending artery graft. Because of persistent exercise symptoms and a nuclear stress test which demonstrated severe ischemia, she returned to the cardiac catheterization laboratory and had successful stenting of the left main coronary artery. Intravascular ultrasound during this procedure demonstrated an intramural course of the left coronary artery.

No renal, skeletal or dermatological abnormalities were reported. Her facial features include bitemporal narrowing, low frontal hairline, short upslanting palpebral fissures, prominent nose, short neck, prominent occiput and low-set, posteriorly rotated ears (Fig. 1c, d). She had a superior pectus carinatum and inferior pectus excavatum.

Table 1 Clinical features of the two probands with biallelic *SMAD6* variants

	Proband 1	Proband 2
Gene	*SMAD6*	*SMAD6*
Mutation and zygosity	p.(Ile466Thr)—homozygous	p.(Phe357Ile) and p.(Ser483Pro)—compound heterozygous
Ethnicity	South Asian	Caucasian
Family history	Younger brother with mild speech development delay	Healthy younger brother and sister
Consanguinity	Yes	No
Gender	Male	Female
Pregnancy	Complicated (IUGR, intraventricular bleeding)	Normal
Birth (weeks)	35 + 4	40
Birth measurements	Weight 2.140 g (− 1.39 *z*), length 44 cm (− 1.72 *z*), OFC 31 cm (− 1.56 *z*)	Weight 3.465 g (− 0.02 *z*), length 49.5 cm (− 1 *z*), OFC n/a
Postnatal course	Hypoglycemia, muscular hypotonia, 5 weeks in NICU	Patent urachus, heart murmur due to pulmonary valve stenosis
Age at last follow-up	6 years	10 years
Measurements at last exam	Weight 21 kg (− 0.46 *z*), length 122 cm (+ 0.26 *z*), OFC 50 cm (− 1.76 *z*)	Weight 37.1 kg (+ 1.01 *z*), length 134 cm (− 0.27 *z*), OFC 51.1 cm (− 0.97 *z*)
Global DD	Present	Absent
ID	Yes	No
Speech delay	Slightly impaired (speaks 3–4 word sentences, uses fantasy language)	No
Milestones	Delayed	Normal
Seizures	No	No
EEG	Dysrhythmic EEG without seizure activity	Not performed
cranial MRI	Normal	A cerebral angiogram showed persistent fetal/embryonic venous channel extending from the superior to the inferior sagittal sinus, but there is no evidence of vascular malformation
Vision	Normal	Normal
Hearing	Normal	Normal
Facial dysmorphism	Microcephaly, deep-set and slightly rotated ears, bushy eyebrows, downslanting palpebral fissures, long nasal bridge, prominent columella	Bitemporal narrowing, low frontal hairline, short upslanting palpebral fissures, prominent nose, short neck, prominent occiput and low-set, posteriorly rotated ears
Cardiac anomalies	Aortic isthmus stenosis, suspected tricuspid aortic valve	Dysplastic and stenotic pulmonic valve, severe left main coronary artery stenosis, mild left pulmonary artery narrowing, dilated cardiomyopathy
Renal anomalies	Unilateral renal hypoplasia	None, normal abdominal ultrasound
Skeletal anomalies	Bilateral radio-ulnar synostosis	None
Skin	Bilateral toe 2/3 syndactyly, very dry and scaly skin	Normal
Other	Hirsutism on the back	Transient neutropenia, hypogammaglobulinemia

DD developmental delay, *EEG* electroencephalogram, *ID* intellectual disability, *IUGR* intrauterine growth retardation, *n/a* not available, *NICU* neonatal intensive care unit, *OFC* occipital frontal head circumference

Prior to undergoing WES, she had a normal chromosome microarray analysis and a normal RASopathy gene panel including sequencing of *BRAF*, *HRAS*, *KRAS*, *PTPN11*, *SOS1*, *MAP2K1*, *MAP2K2*, *SHOC2* and *RAF1*.

Genetic findings

We performed trio or duo WES in a total of 420 pediatric subjects with a neurodevelopmental disorder as described previously (Harms et al. 2018; Hempel et al. 2015). Analysis of WES data was performed according to X-linked, autosomal recessive, and autosomal-dominant inheritance models, the latter with a de novo mutation in the affected child. In a male patient (Proband 1), we identified a homozygous variant in *SMAD6* [with minor allele frequency (MAF) < 0.1% in population databases (dbSNP138, 1000 Genomes Project, Exome Variant Server, ExAC and gnomAD browsers) and no homozygous carriers in the ExAC and gnomAD browsers]: c.1397T > C/p.(Ile466Thr) (Fig. 2a and Table 2). We confirmed the variant in Proband 1 in the homozygous and

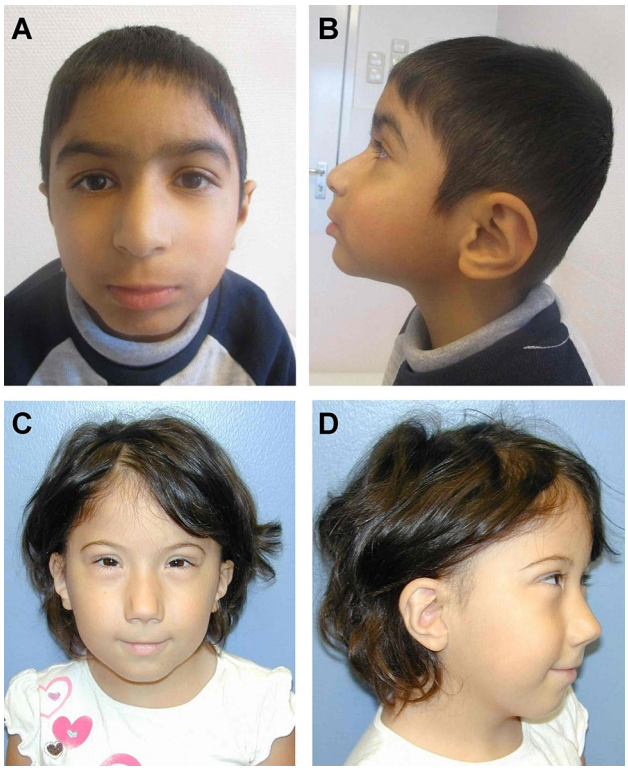

Fig. 1 Facial phenotype of the two probands with biallelic *SMAD6* mutations. Top: Proband 1 at age 5 years, **a** frontal, **b** profile; bottom: Proband 2 at age 4 years, **c** frontal, **d** profile

in his parents in the heterozygous state (data not shown); it was absent in the proband's 3-year-old brother (data not shown) who presented with speech delay.

Through GeneMatcher we identified a second patient (Proband 2) with two heterozygous missense variants in *SMAD6*. Proband 2 carried the de novo variant c.1069T > A/p.(Phe357Ile) and the maternally inherited variant c.1447T > C/p.(Ser483Pro) (Fig. 2a and Table 2). To analyze if the two *SMAD6* variants are present in *cis* or *trans* in Proband 2, we used leukocyte-derived RNA and generated an RT-PCR product spanning *SMAD6* exons 1–4. Direct sequencing of the amplicon confirmed expression of *SMAD6* transcripts with the c.1069T > A variant and those with the c.1447T > C variant in blood (Fig. 2b). Cloning of the RT-PCR product and direct sequencing of a total of six clones revealed two different *SMAD6* transcripts: two cloned mRNAs had the c.1069T > A variant in combination with the wild-type thymine at position c.1447, and four mRNAs showed the normal T allele at c.1069 together with the variant c.1447T > C (Fig. 2c). Together, haplotype determination revealed that the de novo c.1069T > A variant and the maternally inherited variant c.1447T > C were in *trans* in Proband 2.

The *SMAD6* variants p.(Phe357Ile), p.(Ile466Thr) and p.(Ser483Pro) were predicted to impact protein function by three *in silico* tools combining previous pathogenicity scores, with exceptionally high scores; the variants were absent in ExAC and gnomAD browsers (Table 2). The three amino acid substitutions affect residues highly conserved through evolution and invariant among orthologs; they cluster in the functionally important MH2 domain (aa 331–496; Fig. 2a), which is important for binding to activated type I receptors to inhibit TGF-β and BMP signaling (Hanyu et al. 2001). Together, these data suggest that the biallelic *SMAD6* variants detected in Probands 1 and 2 are likely pathogenic and underlie their phenotypes.

Discussion

We report two subjects with biallelic missense variants in *SMAD6* and a complex cardiac phenotype. Proband 1 with the homozygous *SMAD6* variant p.(Ile466Thr) had aortic isthmus stenosis, while the Proband 2 showed a more severe cardiovascular phenotype with a dysplastic and stenotic pulmonary valve, dilated cardiomyopathy, narrowing of the proximal left pulmonary artery and stenosis of the left main coronary artery leading to ischemia and requiring bypass surgery. Proband 2 carried the compound heterozygous *SMAD6* missense variants p.(Phe357Ile) and p.(Ser483Pro). The mutated serine 483 is located in the L3 loop of SMAD6, a 17 amino acid region in the core of the MH2 domain (Fig. 2a). The L3 loop of I-SMADs is required for interaction with type I receptors and for the inhibitory effect of I-SMADs on this receptor type (Kamiya et al. 2010). Highly conserved L3 loops are also present in R-SMADs, such as SMAD2, and specify the SMAD–receptor interactions (Lo et al. 1998). Substitution of serine 433 in SMAD2, corresponding to serine 483 in SMAD6, to alanine (S433A) in the L3 loop has been shown to inhibit SMAD2's association with the receptor (Lo et al. 1998). The data led us to hypothesize that the p.(Ser483Pro) *SMAD6* variant in Proband 2 may decrease the interaction of SMAD6 with type I receptors and diminish the ability of this I-SMAD to inhibit type I receptor signaling. On the other hand, the SMAD6 proteins with a mutation in the MH2 domain might retain certain functions, such as DNA binding.

A role of non-synonymous *SMAD6* variants in cardiovascular disease is further corroborated by three carriers of a heterozygous *SMAD6* mutation who presented with mild to moderate aortic stenosis or coarctation in addition to BAV/TAA (Gillis et al. 2017; Tan et al. 2012). Moreover, mice deficient in Smad6 have cardiovascular anomalies, such as hyperplastic thickening of the valves, elevated blood pressure and perturbed septation of the cardiac outflow tract with for example a narrow ascending aorta and a large pulmonary trunk. Expression of Smad6 has been demonstrated in the outflow tract and atrioventricular cushion regions of

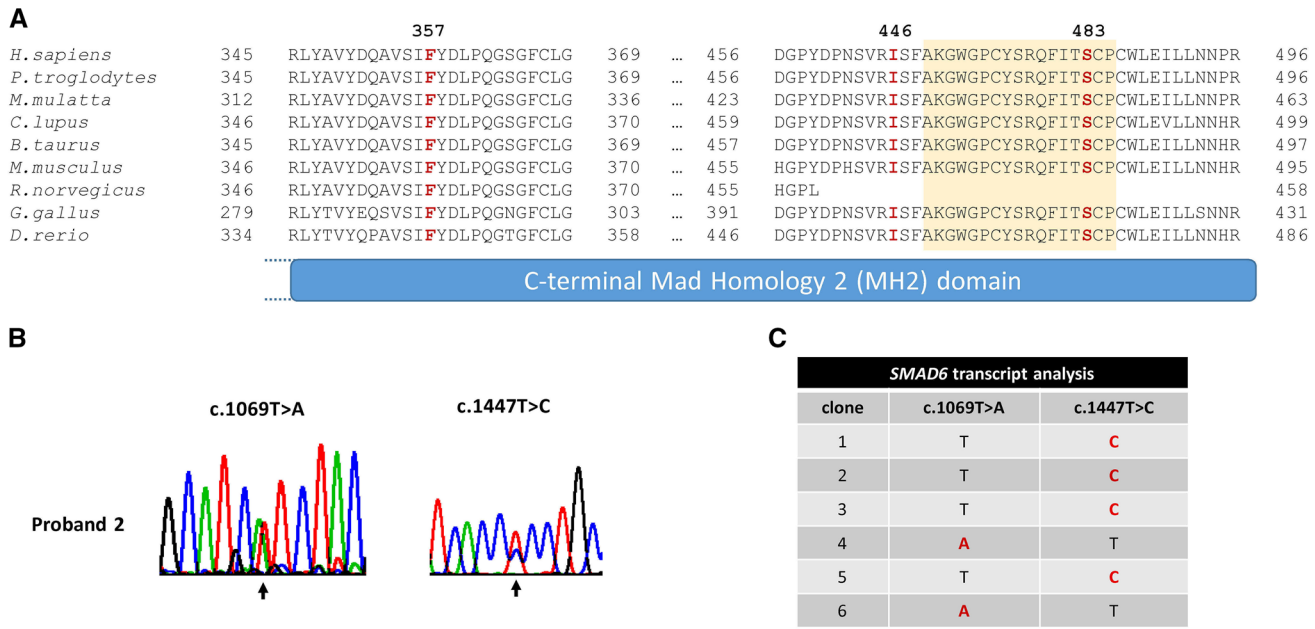

Fig. 2 Localization of *SMAD6* mutations in the MH2 domain and *SMAD6* transcript analysis in Proband 2. **a** Partial amino acid sequence alignments of the human SMAD6 MH2 domain (NP_005576.3) showing evolutionary conservation of the mutated amino acids phenylalanine 357, isoleucine 446 and serine 483 (highlighted in red) between species. Multiple alignments were gathered from https://www.ncbi.nlm.nih.gov/homologene/4079. Amino acids forming the L3 loop, a highly conserved core region in the MH2 domain, are shaded in yellow. **b** Partial sequence electropherograms show the presence of *SMAD6* transcripts with the mutation c.1069T > A (left) and c.1447T > C (right) in leukocyte-derived cDNA of Proband 2. Arrows point to the position of the mutation. **c** RT-PCR, cloning of cDNA-derived amplicons harboring both mutations and sequencing of single colonies were used to determine *SMAD6* haplotypes in Proband 2. Sequence analysis of six cloned PCR products revealed that the proband carries the *SMAD6* mutations in *trans*. A red letter indicates the presence of the mutation in the transcript, and a black letter the wild-type base at the respective position (color figure online)

Table 2 *In silico* pathogenicity prediction and minor allele frequency of biallelic *SMAD6* variants in Probands 1 and 2

Proband	Chr.	Genomic position	Nucleotide change (zygosity) (NM_005585.5)	Amino acid alteration	SMAD6 domain	gnomAD browser: MAF	CADD (> 20)	REVEL (> 0.6)	M-CAP (> 0.025)
1	15	67,073,779	c.1397T > C (hom)	p.(Ile466Thr)	MH2	0	28.8	0.973	0.606
2	15	67,073,451	c.1069T > A (het)	p.(Phe357Ile)	MH2	0	31.0	0.940	0.511
2	15	67,073,829	c.1447T > C (het)	p.(Ser483Pro)	MH2	0	28.9	0.924	0.500

Trio exome data were filtered for potentially pathogenic de novo variants absent in the general population (dbSNP138, 100 Genomes Project, Exome Variant Server, ExAC Browser, and gnomAD Browser) and rare biallelic variants with minor allele frequency (MAF) < 0.1% and no homozygous carriers in the aforementioned databases. The functional impact of the identified variants was predicted by the Combined Annotation Dependent Depletion (CADD) tool, the Rare Exome Variant Ensemble Learner (REVEL) scoring system, and the Mendelian Clinically Applicable Pathogenicity (M-CAP) Score. CADD is a framework that integrates multiple annotations in one metric by contrasting variants that survived natural selection with simulated mutations. Reported CADD scores are phred-like rank scores based on the rank of that variant's score among all possible single nucleotide variants of hg19, with 10 corresponding to the top 10%, 20 at the top 1% and 30 at the top 0.1%. The larger the score, the more likely does the variant have deleterious effects; the score range observed here is strongly supportive of pathogenicity, with all observed variants ranking above ~ 99% of all variants in a typical genome and scoring similarly to variants reported in ClinVar as pathogenic (~ 85% of which score > 15) (Kircher et al. 2014). REVEL is an ensemble method predicting the pathogenicity of missense variants with a strength for distinguishing pathogenic from rare neutral variants with a score ranging from 0 to 1. The higher the score, the more likely is the variant pathogenic (Ioannidis et al. 2016). M-CAP is a classifier for rare missense variants in the human genome, which combines previous pathogenicity scores (including SIFT, Polyphen-2, and CADD), amino acid conservation features and computed scores trained on mutations linked to Mendelian diseases. The recommended pathogenicity threshold is > 0.025 (Jagadeesh et al. 2016)

Chr. chromosome, *het* heterozygous, *hom* homozygous, *MAF* minor allele frequency, *MH2* MAD homology 2

the heart in the developing mouse (Galvin et al. 2000). Preweaning loss of *Smad6*-deficient mice has been noted (Galvin et al. 2000) and was confirmed by others (Estrada et al. 2011; Wylie et al. 2018). Mutant embryos displayed multiple vascular hemorrhages suggesting compromised blood vessel stability that likely accounted for increased embryonic lethality (Wylie et al. 2018). Together, overlapping cardiac abnormalities in *Smad6* knockout mice and individuals with biallelic *SMAD6* variants suggest a role for SMAD6 in the development of the cardiovascular system and developmental angiogenesis. Involvement of Smad6 in angiogenic sprouting and vessel stability (Wylie et al. 2018) might hint at the morphological abnormalities observed in Proband 2, such as the venous anomaly, stenosis of the coronary artery and narrowing of the pulmonary artery. The parents of Probands 1 and 2, who are heterozygous for a pathogenic *SMAD6* variant, are at risk for developing TAA and should be screened regularly for cardiovascular complications.

A two-locus model of inheritance, i.e., the combination of a rare *SMAD6* variant with the C allele of the common SNP *rs1884302*, has been proposed to explain incomplete penetrance of non-syndromic craniosynostosis in carriers of a *SMAD6* variant (Timberlake et al. 2016, 2017). Thus, epistatic interactions between rare *SMAD6* mutations and a common risk allele have been proposed to account for a significant proportion of individuals with non-syndromic midline craniosynostosis (Timberlake et al. 2016, 2017). The heterozygous *SMAD6* variant p.(Ile466Phe) has been detected in an individual with metopic craniosynostosis. A parametric two-locus model was more likely to explain craniosynostosis in this kindred than the one-locus model (see Table S9 in Timberlake et al. 2017). Interestingly, the homozygous variant p.(Ile466Thr) identified in Proband 1 in this study affects the same SMAD6 residue, but causes another amino acid change. Occurrence of two *SMAD6* variants affecting the same codon in individuals with a disease phenotype provides further evidence for pathogenic relevance of these amino acid substitutions. Probands 1 and 2 and their parents did not have craniosynostosis. However, careful examination revealed microcephaly with a flattened forehead in Proband 1 as well as bitemporal narrowing with triangular shape of the forehead and low-set ears in Proband 2 that resemble signs of mild craniosynostosis (Garza and Khosla 2012; Kajdic et al. 2018; Sharma 2013; Twigg and Wilkie 2015). To check for a two-locus model of inheritance, we genotyped the SNP *rs1884302* in Proband 1's family and found the father to be homozygous for the T allele, the mother homozygous for the common risk allele (C) and Proband 1 heterozygous for the risk allele (C/T) (Suppl. Figure 1). Thus, although Proband 1 carried the *SMAD6* variant p.(Ile466Phe) in the homozygous and his mother in the heterozygous state, none of the two individuals who are carriers of the risk allele near *BMP2* had developed typical craniosynostosis. This finding suggests that beside the two-locus pathogenesis, additional genetic and environmental factors likely contribute to the occurrence of non-syndromic craniosynostosis.

Neurodevelopmental evaluation in subjects with craniosynostosis and rare damaging *SMAD6* variants revealed a developmental delay in 73%, suggesting that *SMAD6* mutations may also contribute to neurodevelopmental outcome in heterozygous carriers (Timberlake et al. 2016). Proband 2 in this study showed normal neurodevelopment, whereas Proband 1 presented with mild developmental delay. Although analysis of trio exome data did not reveal any variant that could underlie Proband 1's global developmental delay and mild intellectual disability, we cannot exclude that a second (homozygous) variant could be causal or contributed to his neurological abnormalities.

SMAD6 acts as an inhibitory SMAD and preferentially inhibits BMP signaling. Activation of BMP receptors leads to phosphorylation of the receptor-regulated (R) SMADs 1, 5 and 8, and these R-SMADs form heteromeric complexes with the common-partner SMAD4, translocate to the nucleus and regulate expression of specific target genes (Miyazawa and Miyazono 2017). SMAD6 negatively regulates BMP and also TGF-β signaling in multiple ways (Gomez-Puerto et al. 2019; Wu et al. 2016). BMP signaling is not only important in vascular development and angiogenesis (see above and Cai et al. 2012; Goumans et al. 2018), but also in osteoblast and chondrocyte differentiation (Wu et al. 2016). Chondrocyte-specific expression of Smad6 in mice resulted in postnatal dwarfism and osteopenia. The significantly delayed chondrocyte hypertrophy after birth has been related to impaired bone growth and formation (Horiki et al. 2004). Mice deficient in Smad6 exhibited defects in craniofacial, axial and appendicular skeletal development (Estrada et al. 2011). Together, the data indicate an important role of Smad6 in endochondral bone formation (Estrada et al. 2011; Horiki et al. 2004; Wu et al. 2016). We speculate that compromised SMAD6 function due to mono- or biallelic *SMAD6* mutations may impair inhibition of BMP signaling and result in high osteogenic activity predisposing to craniosynostosis (as suggested by Timberlake et al. 2018). Interestingly, the combination of cardiovascular features and bone overgrowth (e.g. craniosynostosis) has been observed in individuals with autosomal dominant mutations in *TGFBR1*, *TGFBR2*, *SMAD3* or *SKI*, all encoding components of the TGF-β signaling pathway and associated with Loeys–Dietz or Shprintzen–Goldberg syndrome (Cannaerts et al. 2015; Loeys and Dietz 1993; Rodrigues et al. 2009; Schepers et al. 2018). These data suggest that dysregulated TGF-β or BMP signaling due to mutations in components of these pathways can contribute to both cardiovascular and skeletal anomalies in the affected individuals (Kruithof et al. 2012; Wu et al. 2016). Thus, the yet unrecognized

co-occurrence of cardiovascular and craniofacial/skeletal features in individuals with a heterozygous *SMAD6* mutation was likely due to ascertainment bias and suggests that anyone with mono- or biallelic variants in this gene should be screened for both types of disease carefully.

In conclusion, we report two patients with a complex phenotype with overlapping features of cardiac involvement who carry biallelic *SMAD6* missense variants that probably represent hypomorphic alleles. The identification and characterization of more individuals with autosomal recessively inherited *SMAD6* variants are required to define the associated clinical spectrum as biallelic loss-of-function variants or those affecting the MH1 domain may produce similar or a different spectrum of phenotypes. Importantly, in children with more life-threatening or course-determining conditions, such as heart malformations, craniosynostosis is frequently missed. Thus, a more detailed assessment for craniofacial or skeletal anomalies in patients with mono- or biallelic *SMAD6* mutations and cardiac phenotype might be warranted.

Acknowledgements We thank the two probands and family members for their participation in this study and Inka Jantke for skillful technical assistance.

Funding This work was supported by a grant from the Deutsche Forschungsgemeinschaft (KU 1240/10-1 to Ke.K.).

Compliance with ethical standards

Conflict of interest J.J. is an employee of GeneDx, Inc. All other authors declare no competing interests.

References

Bai S, Cao X (2002) A nuclear antagonistic mechanism of inhibitory Smads in transforming growth factor-beta signaling. J Biol Chem 277:4176–4182. https://doi.org/10.1074/jbc.M105105200

Bai S, Shi X, Yang X, Cao X (2000) Smad6 as a transcriptional corepressor. J Biol Chem 275:8267–8270

Braverman AC, Guven H, Beardslee MA, Makan M, Kates AM, Moon MR (2005) The bicuspid aortic valve. Curr Probl Cardiol 30:470–522. https://doi.org/10.1016/j.cpcardiol.2005.06.002

Cai J, Pardali E, Sanchez-Duffhues G, ten Dijke P (2012) BMP signaling in vascular diseases. FEBS Lett 586:1993–2002. https://doi.org/10.1016/j.febslet.2012.04.030

Cannaerts E, van de Beek G, Verstraeten A, Van Laer L, Loeys B (2015) TGF-beta signalopathies as a paradigm for translational medicine. Eur J Med Genet 58:695–703. https://doi.org/10.1016/j.ejmg.2015.10.010

Estrada KD, Retting KN, Chin AM, Lyons KM (2011) Smad6 is essential to limit BMP signaling during cartilage development. J Bone Miner Res 26:2498–2510. https://doi.org/10.1002/jbmr.443

Friedman T, Mani A, Elefteriades JA (2008) Bicuspid aortic valve: clinical approach and scientific review of a common clinical entity. Expert Rev Cardiovasc Ther 6:235–248. https://doi.org/10.1586/14779072.6.2.235

Galvin KM, Donovan MJ, Lynch CA, Meyer RI, Paul RJ, Lorenz JN, Fairchild-Huntress V, Dixon KL, Dunmore JH, Gimbrone MA Jr, Falb D, Huszar D (2000) A role for smad6 in development and homeostasis of the cardiovascular system. Nat Genet 24:171–174. https://doi.org/10.1038/72835

Garg V, Muth AN, Ransom JF, Schluterman MK, Barnes R, King IN, Grossfeld PD, Srivastava D (2005) Mutations in NOTCH1 cause aortic valve disease. Nature 437:270–274. https://doi.org/10.1038/nature03940

Garza RM, Khosla RK (2012) Nonsyndromic craniosynostosis. Semin Plast Surg 26:53–63. https://doi.org/10.1055/s-0032-1320063

Gillis E, Kumar AA, Luyckx I, Preuss C, Cannaerts E, van de Beek G, Wieschendorf B, Alaerts M, Bolar N, Vandeweyer G, Meester J, Wunnemann F, Gould RA, Zhurayev R, Zerbino D, Mohamed SA, Mital S, Mertens L, Bjorck HM, Franco-Cereceda A, McCallion AS, Van Laer L, Verhagen JMA, van de Laar I, Wessels MW, Messas E, Goudot G, Nemcikova M, Krebsova A, Kempers M, Salemink S, Duijnhouwer T, Jeunemaitre X, Albuisson J, Eriksson P, Andelfinger G, Dietz HC, Verstraeten A, Loeys BL, Mibava Leducq C (2017) Candidate gene resequencing in a large bicuspid aortic valve-associated thoracic aortic aneurysm cohort: SMAD6 as an important contributor. Front Physiol 8:400. https://doi.org/10.3389/fphys.2017.00400

Girdauskas E, Borger MA (2013) Bicuspid aortic valve and associated aortopathy: an update. Semin Thorac Cardiovasc Surg 25:310–316. https://doi.org/10.1053/j.semtcvs.2014.01.004

Gomez-Puerto MC, Iyengar PV, Garcia de Vinuesa A, Ten Dijke P, Sanchez-Duffhues G (2019) Bone morphogenetic protein receptor signal transduction in human disease. J Pathol 247:9–20. https://doi.org/10.1002/path.5170

Goto K, Kamiya Y, Imamura T, Miyazono K, Miyazawa K (2007) Selective inhibitory effects of Smad6 on bone morphogenetic protein type I receptors. J Biol Chem 282:20603–20611. https://doi.org/10.1074/jbc.M702100200

Goumans MJ, Zwijsen A, Ten Dijke P, Bailly S (2018) Bone morphogenetic proteins in vascular homeostasis and disease. Cold Spring Harb Perspect Biol 10:a031989. https://doi.org/10.1101/cshperspect.a031989

Guo DC, Gong L, Regalado ES, Santos-Cortez RL, Zhao R, Cai B, Veeraraghavan S, Prakash SK, Johnson RJ, Muilenburg A, Willing M, Jondeau G, Boileau C, Pannu H, Moran R, Debacker J, Bamshad MJ, Shendure J, Nickerson DA, Leal SM, Raman CS, Swindell EC, Milewicz DM, GenTac Investigators NHL, Blood Institute Go Exome Sequencing P, Montalcino Aortic C (2015) MAT2A mutations predispose individuals to thoracic aortic aneurysms. Am J Hum Genet 96:170–177. https://doi.org/10.1016/j.ajhg.2014.11.015

Hanyu A, Ishidou Y, Ebisawa T, Shimanuki T, Imamura T, Miyazono K (2001) The N domain of Smad7 is essential for specific inhibition of transforming growth factor-beta signaling. J Cell Biol 155:1017–1027. https://doi.org/10.1083/jcb.200106023

Harms FL, Kloth K, Bley A, Denecke J, Santer R, Lessel D, Hempel M, Kutsche K (2018) Activating mutations in PAK1, encoding p21-activated kinase 1, cause a neurodevelopmental disorder. Am J Hum Genet 103:579–591. https://doi.org/10.1016/j.ajhg.2018.09.005

Hempel M, Cremer K, Ockeloen CW, Lichtenbelt KD, Herkert JC, Denecke J, Haack TB, Zink AM, Becker J, Wohlleber E, Johannsen J, Alhaddad B, Pfundt R, Fuchs S, Wieczorek D, Strom TM, van Gassen KL, Kleefstra T, Kubisch C, Engels H, Lessel D (2015) De novo mutations in CHAMP1 cause intellectual disability with severe speech impairment. Am J Hum Genet 97:493–500. https://doi.org/10.1016/j.ajhg.2015.08.003

Hinton RB (2012) Bicuspid aortic valve and thoracic aortic aneurysm: three patient populations, two disease phenotypes, and one

shared genotype. Cardiol Res Pract 2012:926975. https://doi.org/10.1155/2012/926975

Horiki M, Imamura T, Okamoto M, Hayashi M, Murai J, Myoui A, Ochi T, Miyazono K, Yoshikawa H, Tsumaki N (2004) Smad6/Smurf1 overexpression in cartilage delays chondrocyte hypertrophy and causes dwarfism with osteopenia. J Cell Biol 165:433–445. https://doi.org/10.1083/jcb.200311015

Ioannidis NM, Rothstein JH, Pejaver V, Middha S, McDonnell SK, Baheti S, Musolf A, Li Q, Holzinger E, Karyadi D, Cannon-Albright LA, Teerlink CC, Stanford JL, Isaacs WB, Xu JF, Cooney KA, Lange EM, Schleutker J, Carpten JD, Powell IJ, Cussenot O, Cancel-Tassin G, Giles GG, MacInnis RJ, Maier C, Hsieh CL, Wiklund F, Catalona WJ, Foulkes WD, Mandal D, Eeles RA, Kote-Jarai Z, Bustamante CD, Schaid DJ, Hastie T, Ostrander EA, Bailey-Wilson JE, Radivojac P, Thibodeau SN, Whittemore AS, Sieh W (2016) REVEL: an ensemble method for predicting the pathogenicity of rare missense variants. Am J Hum Genet 99:877–885. https://doi.org/10.1016/j.ajhg.2016.08.016

Jagadeesh KA, Wenger AM, Berger MJ, Guturu H, Stenson PD, Cooper DN, Bernstein JA, Bejerano G (2016) M-CAP eliminates a majority of variants of uncertain significance in clinical exomes at high sensitivity. Nat Genet 48:1581–1586. https://doi.org/10.1038/ng.3703

Kajdic N, Spazzapan P, Velnar T (2018) Craniosynostosis—recognition, clinical characteristics, and treatment. Bosn J Basic Med Sci 18:110–116. https://doi.org/10.17305/bjbms.2017.2083

Kamiya Y, Miyazono K, Miyazawa K (2010) Smad7 inhibits transforming growth factor-beta family type i receptors through two distinct modes of interaction. J Biol Chem 285:30804–30813. https://doi.org/10.1074/jbc.M110.166140

Kircher M, Witten DM, Jain P, O'Roak BJ, Cooper GM, Shendure J (2014) A general framework for estimating the relative pathogenicity of human genetic variants. Nat Genet 46:310–315. https://doi.org/10.1038/ng.2892

Kruithof BP, Duim SN, Moerkamp AT, Goumans MJ (2012) TGF-beta and BMP signaling in cardiac cushion formation: lessons from mice and chicken. Differentiation 84:89–102. https://doi.org/10.1016/j.diff.2012.04.003

Lewin MB, Otto CM (2005) The bicuspid aortic valve: adverse outcomes from infancy to old age. Circulation 111:832–834. https://doi.org/10.1161/01.CIR.0000157137.59691.0B

Lin X, Liang YY, Sun B, Liang M, Shi Y, Brunicardi FC, Shi Y, Feng XH (2003) Smad6 recruits transcription corepressor CtBP to repress bone morphogenetic protein-induced transcription. Mol Cell Biol 23:9081–9093

Lo RS, Chen YG, Shi Y, Pavletich NP, Massague J (1998) The L3 loop: a structural motif determining specific interactions between SMAD proteins and TGF-beta receptors. EMBO J 17:996–1005. https://doi.org/10.1093/emboj/17.4.996

Loeys BL, Dietz HC (1993) Loeys-Dietz syndrome. In: Adam MP, Ardinger HH, Pagon RA, Wallace SE, Bean LJH, Stephens K, Amemiya A (eds) Gene reviews®. University of Washington, Seattle

Malcic I, Grgat J, Kniewald H, Saric D, Dilber D, Bartonicek D (2015) Bicuspid aortic valve and left ventricular outflow tract defects in children—syndrome of bicuspid aortopathy? Lijec Vjesn 137:267–275

Miyazawa K, Miyazono K (2017) Regulation of TGF-beta family signaling by inhibitory smads. Cold Spring Harb Perspect Biol 9:a022095. https://doi.org/10.1101/cshperspect.a022095

Rauch A, Wieczorek D, Graf E, Wieland T, Endele S, Schwarzmayr T, Albrecht B, Bartholdi D, Beygo J, Di Donato N, Dufke A, Cremer K, Hempel M, Horn D, Hoyer J, Joset P, Ropke A, Moog U, Riess A, Thiel CT, Tzschach A, Wiesener A, Wohlleber E, Zweier C, Ekici AB, Zink AM, Rump A, Meisinger C, Grallert H, Sticht H, Schenck A, Engels H, Rappold G, Schrock E, Wieacker P, Riess O, Meitinger T, Reis A, Strom TM (2012) Range of genetic mutations associated with severe non-syndromic sporadic intellectual disability: an exome sequencing study. Lancet 380:1674–1682. https://doi.org/10.1016/S0140-6736(12)61480-9

Retterer K, Juusola J, Cho MT, Vitazka P, Millan F, Gibellini F, Vertino-Bell A, Smaoui N, Neidich J, Monaghan KG, McKnight D, Bai R, Suchy S, Friedman B, Tahiliani J, Pineda-Alvarez D, Richard G, Brandt T, Haverfield E, Chung WK, Bale S (2016) Clinical application of whole-exome sequencing across clinical indications. Genet Med 18:696–704. https://doi.org/10.1038/gim.2015.148

Rodrigues VJ, Elsayed S, Loeys BL, Dietz HC, Yousem DM (2009) Neuroradiologic manifestations of Loeys-Dietz syndrome type 1. AJNR Am J Neuroradiol 30:1614–1619. https://doi.org/10.3174/ajnr.A1651

Schepers D, Tortora G, Morisaki H, MacCarrick G, Lindsay M, Liang D, Mehta SG, Hague J, Verhagen J, van de Laar I, Wessels M, Detisch Y, van Haelst M, Baas A, Lichtenbelt K, Braun K, van der Linde D, Roos-Hesselink J, McGillivray G, Meester J, Maystadt I, Coucke P, El-Khoury E, Parkash S, Diness B, Risom L, Scurr I, Hilhorst-Hofstee Y, Morisaki T, Richer J, Desir J, Kempers M, Rideout AL, Horne G, Bennett C, Rahikkala E, Vandeweyer G, Alaerts M, Verstraeten A, Dietz H, Van Laer L, Loeys B (2018) A mutation update on the LDS-associated genes TGFB2/3 and SMAD2/3. Hum Mutat 39:621–634. https://doi.org/10.1002/humu.23407

Sharma RK (2013) Craniosynostosis. Indian J Plast Surg 46:18–27. https://doi.org/10.4103/0970-0358.113702

Tan HL, Glen E, Topf A, Hall D, O'Sullivan JJ, Sneddon L, Wren C, Avery P, Lewis RJ, ten Dijke P, Arthur HM, Goodship JA, Keavney BD (2012) Nonsynonymous variants in the SMAD6 gene predispose to congenital cardiovascular malformation. Hum Mutat 33:720–727. https://doi.org/10.1002/humu.22030

Timberlake AT, Choi J, Zaidi S, Lu Q, Nelson-Williams C, Brooks ED, Bilguvar K, Tikhonova I, Mane S, Yang JF, Sawh-Martinez R, Persing S, Zellner EG, Loring E, Chuang C, Galm A, Hashim PW, Steinbacher DM, DiLuna ML, Duncan CC, Pelphrey KA, Zhao H, Persing JA, Lifton RP (2016) Two locus inheritance of non-syndromic midline craniosynostosis via rare SMAD6 and common BMP2 alleles. Elife 5:e20125. https://doi.org/10.7554/elife.20125

Timberlake AT, Furey CG, Choi J, Nelson-Williams C, Loring E, Galm A, Kahle KT, Steinbacher DM, Larysz D, Persing JA, Lifton RP, Yale Center for Genome A (2017) De novo mutations in inhibitors of Wnt, BMP, and Ras/ERK signaling pathways in non-syndromic midline craniosynostosis. Proc Natl Acad Sci USA 114:E7341–E7347. https://doi.org/10.1073/pnas.1709255114

Timberlake AT, Wu R, Nelson-Williams C, Furey CG, Hildebrand KI, Elton SW, Wood JS, Persing JA, Lifton RP (2018) Co-occurrence of frameshift mutations in SMAD6 and TCF12 in a child with complex craniosynostosis. Hum Genome Var 5:14. https://doi.org/10.1038/s41439-018-0014-x

Twigg SR, Wilkie AO (2015) A genetic-pathophysiological framework for craniosynostosis. Am J Hum Genet 97:359–377. https://doi.org/10.1016/j.ajhg.2015.07.006

Tzemos N, Therrien J, Yip J, Thanassoulis G, Tremblay S, Jamorski MT, Webb GD, Siu SC (2008) Outcomes in adults with bicuspid aortic valves. JAMA 300:1317–1325. https://doi.org/10.1001/jama.300.11.1317

Vallely MP, Semsarian C, Bannon PG (2008) Management of the ascending aorta in patients with bicuspid aortic valve disease. Heart Lung Circ 17:357–363. https://doi.org/10.1016/j.hlc.2008.01.007

Wu M, Chen G, Li YP (2016) TGF-beta and BMP signaling in osteoblast, skeletal development, and bone formation, homeostasis

and disease. Bone Res 4:16009. https://doi.org/10.1038/boneres.2016.9

Wylie LA, Mouillesseaux KP, Chong DC, Bautch VL (2018) Developmental SMAD6 loss leads to blood vessel hemorrhage and disrupted endothelial cell junctions. Dev Biol 442:199–209. https://doi.org/10.1016/j.ydbio.2018.07.027